

Retrospective Study

Baseline metabolites could predict responders with hepatitis B virus-related liver fibrosis for entecavir or combined with FuzhengHuayu tablet

Yun-Kai Dai, Hai-Na Fan, Kai Huang, Xin Sun, Zhi-Min Zhao, Cheng-Hai Liu

Specialty type: Gastroenterology and hepatology**Provenance and peer review:**

Unsolicited article; Externally peer reviewed.

Peer-review model: Single blind**Peer-review report's scientific quality classification**Grade A (Excellent): 0
Grade B (Very good): B
Grade C (Good): C
Grade D (Fair): 0
Grade E (Poor): 0**P-Reviewer:** Kao JT, Taiwan;
Kishida Y, Japan**Received:** June 8, 2023**Peer-review started:** June 8, 2023**First decision:** August 5, 2023**Revised:** August 21, 2023**Accepted:** September 14, 2023**Article in press:** September 14, 2023**Published online:** September 27, 2023**Yun-Kai Dai, Hai-Na Fan, Xin Sun, Zhi-Min Zhao, Cheng-Hai Liu**, Shuguang Hospital Affiliated to Shanghai University of Traditional Chinese Medicine, Institute of Liver Diseases, Shanghai 201203, China**Kai Huang, Xin Sun, Zhi-Min Zhao, Cheng-Hai Liu**, Shanghai Key Laboratory of Traditional Chinese Clinical Medicine, Institute of Liver Diseases, Shanghai 201203, China**Cheng-Hai Liu**, Key Laboratory of Liver and Kidney Diseases, Institute of Liver Diseases, Shanghai 201203, China**Corresponding author:** Cheng-Hai Liu, MD, PhD, Director, Doctor, Professor, Shuguang Hospital Affiliated to Shanghai University of Traditional Chinese Medicine, Institute of Liver Diseases, No. 528 Zhangheng Road, Pudong New Area, Shanghai 201203, China.
chenghai.liu@shutcm.edu.cn**Abstract****BACKGROUND**

After receiving entecavir or combined with FuzhengHuayu tablet (FZHY) treatment, some sufferers with hepatitis B virus (HBV)-related liver fibrosis could achieve a histological improvement while the others may fail to improve even worsen. Serum metabolomics at baseline in these patients who were effective in treatment remain unclear.

AIM

To explore baseline serum metabolites characteristics in responders.

METHODS

A total of 132 patients with HBV-related liver fibrosis and 18 volunteers as healthy controls were recruited. First, all subjects were divided into training set and validation set. Second, the included patients were subdivided into entecavir responders (E-R), entecavir no-responders (E-N), FZHY + entecavir responders (F-R), and FZHY + entecavir no-responders (F-N) following the pathological histological changes after 48 wk' treatments. Then, Serum samples of all subjects before treatment were tested by high performance liquid chromatography-tandem mass spectrometry (LC-MS) high-performance LC-MS. Data processing was conducted using multivariate principal component analysis and orthogonal

partial least squares discriminant analysis. Diagnostic tests of selected differential metabolites were used for Boruta analyses and logistic regression.

RESULTS

As for the intersection about differential metabolic pathways between the groups E-R *vs* E-N and F-R *vs* F-N, results showed that 4 pathways including linoleic acid metabolism, aminoacyl-tRNA biosynthesis, cyanoamino acid metabolism, alanine, aspartate and glutamate metabolism were screened out. As for the differential metabolites, these 7 intersected metabolites including hydroxypropionic acid, tyrosine, citric acid, taurochenodeoxycholic acid, benzoic acid, 2-Furoic acid, and propionic acid were selected.

CONCLUSION

Our findings showed that 4 metabolic pathways and 7 differential metabolites had potential usefulness in clinical prediction of the response of entecavir or combined with FZHY on HBV fibrotic liver.

Key Words: Serum metabolomics; Differential metabolites; Therapeutic responders; Entecavir; FuzhengHuayu tablet; Hepatitis B virus-related liver fibrosis

©The Author(s) 2023. Published by Baishideng Publishing Group Inc. All rights reserved.

Core Tip: This study will use high-performance liquid chromatography-tandem mass spectrometry and multivariate statistical modelings to predict serum metabolites of the treatment (entecavir or entecavir + FuzhengHuayu tablet) that effectively reversed hepatitis B virus-related liver fibrosis. It is of great theoretical and practical significance to prevent the transformation of liver fibrosis to cirrhosis or even hepatocellular carcinoma and reduce the social burden.

Citation: Dai YK, Fan HN, Huang K, Sun X, Zhao ZM, Liu CH. Baseline metabolites could predict responders with hepatitis B virus-related liver fibrosis for entecavir or combined with FuzhengHuayu tablet. *World J Hepatol* 2023; 15(9): 1043-1059

URL: <https://www.wjgnet.com/1948-5182/full/v15/i9/1043.htm>

DOI: <https://dx.doi.org/10.4254/wjh.v15.i9.1043>

INTRODUCTION

Liver fibrosis, characterized by the progressive and reversible accumulation of fibrillar extracellular matrix components in the liver, poses a significant threat to the physiological architecture of the liver and accounts for nearly half of all-cause mortality associated with various liver diseases worldwide[1-2]. Among the numerous causes of acute and chronic liver diseases, hepatitis B virus (HBV) infection stands out as a prevalent culprit and a leading instigator of liver fibrosis[3]. Epidemiological studies have revealed that more than 240 million individuals are afflicted by HBV infection[4]. Given the insidious nature of chronic hepatitis B (CHB), it can swiftly advance to fibrosis, cirrhosis, or even hepatocellular carcinoma (HCC) if left unchecked[5]. Hence, it is imperative to consider the use of antiviral agents in the treatment of HBV, with entecavir serving as a prominent representative.

In recent years, the study of liver fibrosis has consistently been a focal point of medical research[6]. Serving as a reversible lesion, liver fibrosis acts as the intermediary stage between the development of chronic liver diseases and the progression to cirrhosis[7]. Presently, effective treatments for cirrhosis remain limited, underscoring the significance of anti-liver fibrosis as a crucial therapeutic strategy. FuzhengHuayu tablet (FZHY), a novel traditional Chinese medicine (TCM) remedy, has gained widespread usage in clinical practice for the treatment of liver fibrosis and cirrhosis[8]. Furthermore, our prior multi-center clinical investigation has substantiated that entecavir + FZHY therapy significantly enhances the histological reversal rate of CHB fibrosis[9]. Nonetheless, approximately one-third of patients fail to exhibit a substantial histological response[10]. Consequently, elucidating the biological characteristics of individuals who respond to entecavir or entecavir + FZHY will undoubtedly contribute to the enhancement of precision therapy's therapeutic efficacy.

To date, no single biomarker or scoring system has achieved the ideal balance of sensitivity and specificity for the detection and characterization of liver fibrosis[11]. While liver biopsy remains the gold standard for staging liver fibrosis, it is burdened by limitations such as invasiveness, sampling errors, and the potential for complications[12]. Furthermore, this method lacks convenience in tracking the dynamic progression of liver fibrosis and assessing therapeutic outcomes. Fortunately, non-invasive diagnostic techniques for liver fibrosis, including transient elastography (Fibroscan), elastography, and diffusion-weighted magnetic resonance imaging, have made significant advancements and gained widespread clinical utility. However, these approaches are susceptible to interference from factors such as a patient's body mass index (BMI), liver inflammation, or hepatocyte degeneration[13].

Metabolomics, an emerging field following in the footsteps of genomics, transcriptomics, and proteomics, represents a novel approach to systematically study changes in small-molecule metabolites produced by the body's metabolism[14]. Often referred to as the "end point" of the genome and proteome, metabolomics allows for the comprehensive analysis of

various metabolites and their metabolic pathways in a population, offering high-throughput and modeling capabilities. Furthermore, metabolomics can unveil downstream products of gene and protein expression within an organism, providing insight into all physiological processes within the body. Due to its close proximity to disease phenotypes, metabolomics is particularly well-suited for disease classification and biomarker discovery. In this study, we intend to employ high-performance liquid chromatography-mass spectrometry (HPLC-MS) and advanced multivariate statistical modeling to predict serum metabolite profiles associated with the effective reversal of HBV-related liver fibrosis induced by treatment with entecavir or entecavir + FZHY. This research holds profound theoretical and practical significance in preventing the progression of liver fibrosis to cirrhosis or HCC, thereby reducing the societal burden associated with these conditions.

MATERIALS AND METHODS

Patient selection

This is a cross-sectional study that encompasses multi-center randomized controlled clinical trials. We enrolled a total of 132 patients with HBV-related liver fibrosis, along with 18 healthy volunteers as controls, during the period from September 9, 2014, to October 25, 2018. The study comprised two distinct sets: A training set and a validation set. All participants were recruited from 20 hospitals across China and provided voluntary informed consent. The research protocol received ethical approval from the Ethics Committee of Shuguang Hospital Affiliated with Shanghai University of TCM (ethical approval number: 2014-331-27-01). The diagnostic criteria for HBV-related liver fibrosis were in accordance with the guidelines for the prevention and treatment of CHB (2019)[15]. The primary focus of this study was on the progression of liver fibrosis, assessed primarily through liver histopathology using the Ishak scoring system as the indicator for therapeutic evaluation. The primary outcome measured was the proportion of patients demonstrating a 1-point improvement in liver fibrosis stage, as per the Ishak score, from baseline to 48 wk. Liver biopsies were performed both before and 48 wk after the initiation of combination TCM treatment, and the histopathological evaluation was independently conducted by three pathologists. Fibrosis regression was defined as a decrease in the Ishak score of 1 or greater[16]. The final fibrotic scores were established based on consensus among two or more pathologists; any disagreements were resolved by a central pathologist. However, a detailed assessment of inflammation levels was not performed. For the noninvasive diagnosis and staging of liver fibrosis, aminotransferase-to-platelet ratio index (APRI) and fibrosis index based on the 4 factor (FIB-4) were primarily employed as adjunct diagnostic tools to assess the severity of liver fibrosis. Consequently, the two treatment groups were further subdivided into four subgroups: Entecavir responders (E-R), entecavir non-responders (E-N), FZHY + entecavir responders (F-R), and FZHY + entecavir non-responders (F-N). Inclusion criteria for this study encompassed individuals aged 18 years or older who met the aforementioned diagnostic criteria. Exclusion criteria included the following: individuals with liver fibrosis not associated with HBV infection; those with cardio-cerebrovascular or infectious diseases or other digestive system disorders; pregnant or lactating women; and patients with poor compliance.

Sample collection

All subjects were asked to have normal regular diets and schedules on the day before blood collection, and venous blood was collected on an empty stomach the next morning. 500 μ L serum was centrifuged at 4 °C at 4000 r/min and stored in a -80 °C for later use.

Sample processing

The cryopreserved serum was thawed on ice-bath in case of degradation. 25 μ L of serum was added to a 96-well plate for the transferring to the Biomek 4000 workstation (Biomek 4000, Beckman Coulter, Inc., Brea, CA, United States). 120 μ L of methanol was automatically added to each serum and vortexed for 5 min. The plate was centrifuged at 4000 g for half an hour and it was returned back to the workstation. 30 μ L of supernatant fluid was transferred to a clean 96-well plate, where each well was filled with 20 μ L of freshly prepared derivative reagents. Then the plate was sealed for derivatization at 30 °C for an hour and the sample was diluted by 330 μ L of ice-cold 50% methanol solution. Next, the plate was left at -20 °C for 20 min and centrifuged at 4 °C for half an hour. Finally, 135 μ L of supernatant fluid was taken to a new 96-well plate, which was sealed for liquid chromatography-tandem mass spectrometry (LC-MS) analysis.

Quality control analysis

All samples were mixed into one quality control sample for quality control. The quality control samples were analyzed 6 times and randomly respectively tested 2 times before, during and after analysis. The total ion flow chromatograms of the quality control samples were overlapped and the total principal component analysis (PCA) was performed. It would show good repeatability if the results of the quality control samples were close to each other.

Materials and reagents

Formic acid (Optima grade) was obtained from Sigma-Aldrich (St. Louis, MO, United States). Methanol (Optima LC-MS) and acetonitrile (Optima LC-MS) were purchased from Thermo-Fisher Scientific (FairLawn, NJ, United States). The experimental water was distilled water.

Instrument analysis platform

We used a ultra-performance liquid chromatography coupled to tandem mass spectrometry system (ACQUITY UPLC-Xevo TQ-S, Waters Corp., Milford, MA, United States) in order to quantitate all targeted metabolites in this study. A briefly description of the optimized instrument settings can be shown in [Supplementary Table 1](#). Meanwhile, the instrument performance optimization and routine maintenance were conducted every week.

LC-MS analysis

Extraction of ion flow chromatograms based on HPLC-MS. (1) Chromatographic elution gradient: The initial gradients were 5% solution B (acetonitrile + 0.1% formic acid) and 95% solution A (distilled water + 0.1% formic acid), whose elution time lasted 2-10 min. Meanwhile, solution B increased linearly to 95% for 5 min and then dropped back to 5%. The injection volume was 4 μ L and the automatic sampler temperature was 4 $^{\circ}$ C; and (2) mass spectrometry scanning mode: Positive and negative ions were used for detection by mass spectrometry. The ion scanning time was 0.03 s, the time interval was 0.02 s, and the data collection range was 50-100 m/z .

Screening and identification of potential metabolites

The data of group A and group B were analyzed by total PCA, then partial least squares discriminant analysis (PLS-DA) was used, and finally the supervised orthogonal PLS-DA (OPLS-DA) was used for modeling analysis. Variable importance in the projection (VIP) values (threshold > 1) based on the OPLS-DA model, combined with P value ($P < 0.05$) of t test, were used to find metabolites which were differentially expressed. Potential metabolites were identified by searching online database (<http://metlin.scripps.edu/>) to compare the mass charge ratio or molecular mass of mass spectrometry.

Potential metabolite enrichment analysis and metabolic pathway analysis

Metabo-Analyst online analysis software (<https://www.metaboanalyst.ca>) and Kyoto Encyclopedia of Genes and Genomes databases (<https://www.kegg.jp/>) were used for metabolic pathway analysis and enrichment analysis of the identified potential metabolites so as to determine the metabolic pathways involved in the potential metabolites, and to evaluate the diagnostic performance of the potential metabolites enriched in pathways.

Diagnostic tests

In order to validate the applicability and stability of the selected differential metabolites, random forest (RF), Support vector machine (SVM) and Boruta analyses were conducted for each selected metabolite in sequence. Boruta analysis, the maximum number of runs with 1000, was an RF-based feature selection method that it selects key features with more significant distinguishing ability than random lag features. When provisional features were included, a secondary selection was made to determine whether certain metabolites with large fluctuations should be included in the selected features.

These differential metabolites used for subsequent model construction were modeled and predicted using logistic regression. After modeling, sensitivity and specificity values were calculated to evaluate the model effects through drawing the receiver operating characteristic curve. Meanwhile, the closer the area under the curve (AUC) value is to 1, the better the sensitivity, specificity and diagnostic abilities. The conventional AUC of metabolites with the value ≥ 0.75 indicated relatively good sensitivity and specificity.

Statistical analysis

Statistical analysis software packages in R studio (<http://cran.r-project.org/>) were performed for the statistical algorithms. All the included data were calculate with mean \pm SD or median-interquartile range. The Mann-Whitney U test or t test was used for the statistical differences in pairwise comparison. Multivariate statistical modelings including PCA, PLS-DA, and OPLS-DA were used for the multi-class classification and identification of differently altered metabolites. Among these modelings, each spatial dot in the K-dimensional space represented an individual sample with the samples color-coded based on grouping information. R^2X and R^2Y respectively represented the fraction of the variance of X matrix and Y matrix, while Q^2Y represented the predictive accuracy of the model. Cumulative values of R^2X and R^2Y approaching 1.0, along with Q^2Y greater than 0.2 (permutation test), indicated a model with a satisfactory predictive ability. Those variables with VIP greater than 1.0 are considered significantly different between classes. If multidimensional statistics cannot establish a robust discriminant model (such as uneven distribution of inter-group sample categories or large intra-group deviation), differential metabolites between the two groups would be acquired with the aid of univariate analysis.

RESULTS

Baseline clinical characteristics of participants

In the training set, there were 23 sufferers in each subgroup and 13 normal volunteers as control. In the validation set, there were 10 patients in each subgroup and 5 volunteers as control. Details of the baseline clinical characteristics of the two datasets can be found in [Table 1](#). Specifically, there were no significant differences in the gender, age, BMI, alanine aminotransferase, aspartate aminotransferase, albumin (ALB), total bilirubin (TBIL), creatinine, prothrombin time, platelet count, alpha fetoprotein, FIB-4, aspartate APRI, Ishak score in the training set ($P > 0.05$). However, in the

Table 1 Demographic and clinical data of patients and volunteers in training set and validation set

	Training set (n = 105)					Validation set (n = 45)				
	F-R (n = 23)	F-N (n = 23)	E-R (n = 23)	E-N (n = 23)	NOR (n = 13)	F-R (n = 10)	F-N (n = 10)	E-R (n = 10)	E-N (n = 10)	NOR (n = 5)
Male/Female	15/8	15/8	16/7	17/6	9/4	7/3	10/0	6/4	8/2	4/1
Age (yr)	44.17 ± 6.25	42.43 ± 8.36	40.65 ± 7.73	42.22 ± 7.97	36.92 ± 6.18	42.80 ± 5.01	38.10 ± 11.95	45.00 ± 7.93	47.40 ± 10.44	37.80 ± 8.79
BMI (kg/m ²)	23.60 ± 2.56	23.64 ± 3.17	23.54 ± 2.06	23.92 ± 2.73	24.20 ± 1.34	23.22 ± 3.30	24.76 ± 1.65	24.61 ± 2.29	23.16 ± 3.86	22.60 ± 1.71
ALT (IU/L)	42.52 ± 29.59	41.03 ± 20.48	68.91 ± 89.81	47.34 ± 27.83	/	49.80 ± 50.83	48.80 ± 33.14	57.08 ± 46.97	58.33 ± 73.02	/
AST (IU/L)	40.50 ± 21.35	41.80 ± 19.41	53.47 ± 51.20	50.53 ± 27.59	/	38.71 ± 16.39	47.75 ± 28.32	77.64 ± 120.70	48.73 ± 35.54	/
ALB (IU/L)	43.84 ± 5.50	41.43 ± 6.07	43.51 ± 5.75	42.22 ± 4.61	/	42.40 ± 5.08	35.70 ± 6.67	39.68 ± 5.95	41.53 ± 4.64	/
TBIL (μmol/L)	16.15 ± 10.88	13.27 ± 6.36	13.36 ± 9.25	14.16 ± 6.51	/	11.98 ± 4.90	24.49 ± 16.83	22.08 ± 13.61	12.18 ± 5.79	/
Cr (μmol/L)	64.43 ± 17.03	66.39 ± 11.99	69.57 ± 16.59	64.57 ± 14.67	/	72.80 ± 18.27	71.10 ± 9.71	65.80 ± 13.70	83.60 ± 25.07	/
PT (S)	13.22 ± 1.48	13.23 ± 1.41	13.31 ± 1.46	13.78 ± 1.52	/	13.21 ± 1.32	14.27 ± 2.90	14.10 ± 1.33	13.88 ± 1.83	/
PLT (× 10 ⁹ /L)	119.02 ± 49.99	113.47 ± 61.33	131.70 ± 49.26	104.65 ± 41.65	/	145.10 ± 64.42	112.00 ± 36.18	98.88 ± 45.13	106.40 ± 37.97	/
AFP (ng/ml)	23.70 ± 59.55	12.46 ± 13.22	18.63 ± 42.03	14.75 ± 15.56	/	16.73 ± 31.93	54.81 ± 93.15	25.25 ± 41.79	14.86 ± 15.91	/
FIB-4	2.99 ± 2.06	3.31 ± 2.38	2.54 ± 1.62	3.46 ± 1.75	/	2.29 ± 1.95	2.72 ± 1.51	5.63 ± 8.14	3.55 ± 1.89	/
APRI	1.10 ± 0.96	1.23 ± 0.95	1.40 ± 1.60	1.31 ± 0.73	/	0.81 ± 0.54	1.18 ± 0.84	3.17 ± 6.23	1.28 ± 0.92	/
Ishak score	5.48 ± 0.51	5.43 ± 0.51	5.35 ± 0.49	5.39 ± 0.50	/	5.40 ± 0.52	5.40 ± 0.52	5.50 ± 0.53	5.10 ± 0.32	/

BMI: Body mass index; ALT: Alanine aminotransferase; AST: Aspartate aminotransferase; ALB: Albumin; TBIL: Total bilirubin; Cr: Creatinine; PT: Prothrombin time; PLT: Platelet count; AFP: Alpha fetoprotein; FIB-4: Fibrosis index based on the 4 factor; APRI: Aspartate aminotransferase-to-platelet ratio index; E-R: Entecavir responders; E-N: Entecavir no-responders; F-R: FuzhengHuayu tablet + entecavir responders; F-N: FuzhengHuayu tablet + entecavir no-responders; NOR: Normal.

validation set, the serum ALB and TBIL levels significantly differed between the F-R and F-N patients ($P < 0.05$), but the other indexes were not statistically significant ($P > 0.05$).

The pathological histological results of the liver biopsy

The obtained tissues *via* liver biopsy were fixed in 10% formalin and embedded in paraffin. Sections of each liver tissue were cut and stained using hematoxylin-eosin (HE) staining for histopathological analysis. Based on the HE staining results and Ishak score, staging of liver fibrosis was determined as F1 to F6[17]. Briefly, F1: Some portal areas have fibrosis but no fibrous septum; F2: Many portal areas have fibrosis along with one fibrous septum; F3: Many portal areas have fibrosis along with two or three fibrous septa; F4: Portal areas have obvious portal-junction bridge fibrosis along with more than four fibrous septa; F5: Portal areas have obvious portal-junction bridge fibrosis or portal-central bridge fibrosis along with one to three pseudolobuli and F6: More than three pseudolobuli. Details of relevant figures can be found in [Supplementary Figure 1](#).

Overall metabolomics analysis of serum samples

Representative nuclear magnetic resonance spectra with targeted metabolites are exhibited in [Supplementary Figure 2](#). The serum spectra included high-intensity signals from Maleic acid, Glycine (G1 *vs* G2), dihomo-gamma-linolenic acid, arachidonic acid, hydroxypropionic acid, (G3 *vs* G4), 2-Furoic acid, 2-Phenylpropionate, arachidonic acid, benzoic acid, butyric acid, aconitic acid, citric acid, dimethylglycine, glycochenodeoxycholic acid (GCDCA), homovanillic acid, hydrocinnamic acid, hydroxyphenyllactic acid, isocitric acid, tyrosine, phenyllactic acid, propionic acid, taurochenodeoxycholic acid (TCDC), tricarboxylic acid (TCA) (G9 *vs* G1-G4). Because all patients were suffered from HBV-related

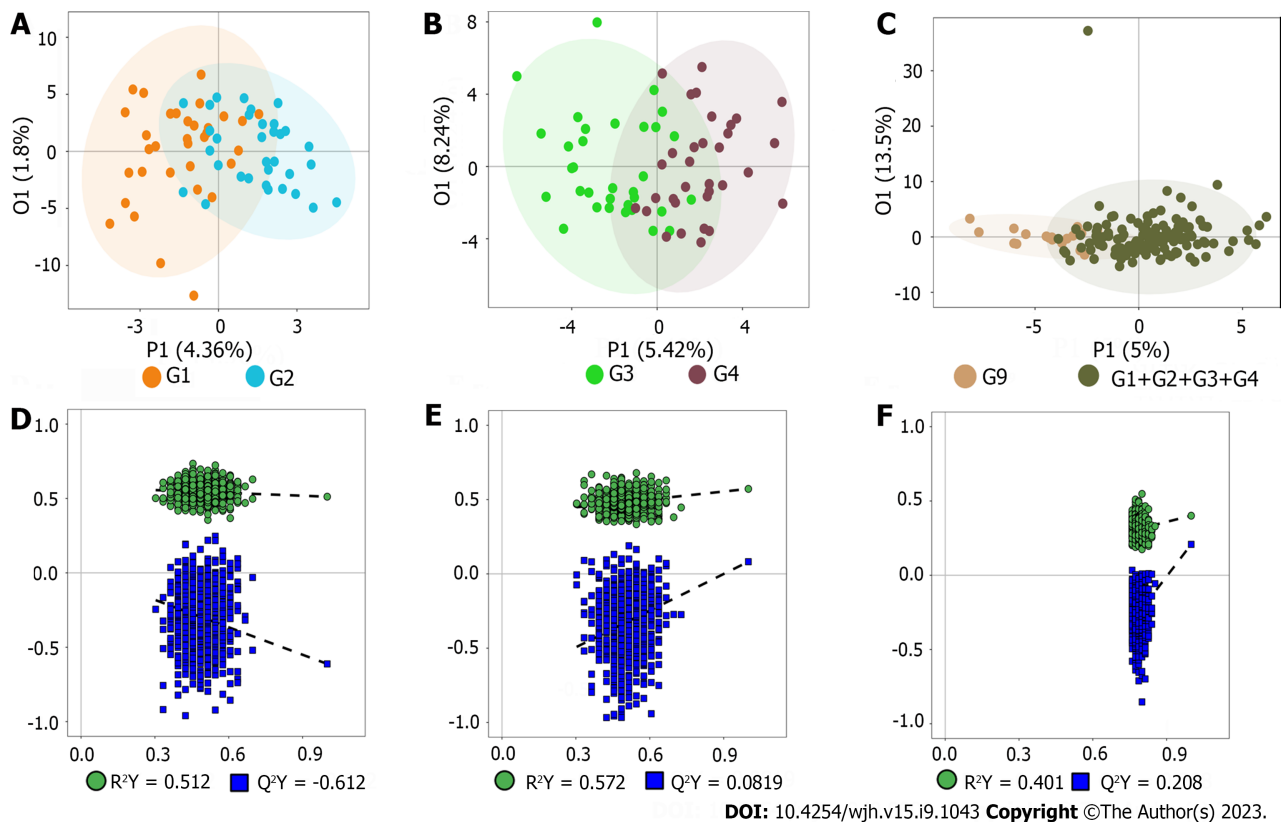


Figure 1 Orthogonal partial least squares discriminant analysis of all the metabolites. A: Score of entecavir responders (E-R) vs entecavir non-responders (E-N); B: Score of FuzhengHuayu tablet (FZHY) + entecavir responders (F-R) vs FZHY + entecavir non-responders (F-N); C: Score of patients vs volunteers; D: R^2X and R^2Y of E-R vs E-N; E: R^2X and R^2Y of F-R vs F-N; F: R^2X and R^2Y of patients vs volunteers.

liver fibrosis in this study, statistical assessment by PCA indicated not clear separation in each group (E-R vs E-N; F-R vs F-N; patients vs volunteers) (Supplementary Figure 3). Besides, in order to exclude the possible confounding factors irrelevant to the group differences and to assess the statistical meaning of those signals, OPLS-DA was conducted and the result showed that the discrimination model could differentiate the two groups despite within a small overlap in one orthogonal component (Figure 1A-C). Moreover, as shown in Figure 1D-F, the models with $R^2(Y)$ of 0.512 (E-R vs E-N), 0.572 (F-R vs F-N), 0.401 (patients vs volunteers) suggested relatively good predictability and no potential over-fit. However, the models with $Q^2(Y)$ of -0.612 (E-R vs E-N), 0.0819 (F-R vs F-N), and 0.208 (patients vs volunteers) indicated the potential risk of over-fit.

Serum metabolites relevant to responders and HBV-related liver fibrosis

Due to the possibility of potential risk of the over-fit in these models, differential metabolites between the two groups were acquired with the aid of univariate analysis instead of analysis together with the VIP values from the above OPLS-DA model. Furthermore, in order to explore the applicability and stability of the distinctive models, serum samples from all the included patients and volunteers were collected and analyzed using the training set and validation set for the subsequent analyses.

In order to find out potential metabolites involving in responders and HBV-related liver fibrosis among the thousands of variables, a pairwise comparison in each group was conducted. According to the threshold value ($P < 0.05$ and $|\log_2FC| \geq 0$, FC: Fold change), a total of 2 (E-R vs E-N), 16 (F-R vs F-N) and 35 (patients vs volunteers) potential metabolites in the training set (Figure 2A-C) were obtained while a total of 8 (E-R vs E-N), 7 (F-R vs F-N) and 23 (patients vs volunteers) potential metabolites in the validation set (Figure 2D-F) were acquired.

Selection of potential metabolites in different sets

By taking intersection and union set in terms of the aforementioned obtained unidimensional and multidimensional potential metabolites, these metabolites that may have biological significance can be selected on the basis of OPLS-DA ($VIP > 1$) and univariate ($P < 0.05$ and $|\log_2FC| \geq 0$) analyses. A total of 53 potential metabolites in the training set and 38 potential metabolites in the validation set were obtained. Detailed information of these selected potential metabolites were shown in Table 2. The distribution of data for all the metabolites in each group can be found in Supplementary Figure 4. Furthermore, a heat map, together with Z-score, was used for analysis of these selected metabolites and the results suggested that the pairwise comparisons between the two groups could be separated no matter which data set was (Figure 3).

Table 2 The selected potential metabolites in training set and validation set

Class	HMDB	KEGG	Metabolite	Uni_P	Uni_FDR	FC	log2FC	OPLSDA_VIP
Training set								
Fatty acids	HMDB0000448	C06104	Adipic acid	0.03	1.00	0.77	-0.37	1.65
Organic acids	HMDB0000176	C01384	Maleic acid	0.04	1.00	0.84	-0.25	1.73
Fatty acids	HMDB0060038	NA	10Z-Heptadecenoic acid	0.01	0.31	3.10	1.63	1.90
	HMDB0002925	C03242	Dihomo-gamma-linolenic acid	0.02	0.32	2.08	1.05	1.60
	HMDB0001043	C00219	Arachidonic acid	0.04	0.44	1.70	0.76	1.79
	HMDB0002183	C06429	DHA	0.02	0.32	1.85	0.89	2.03
	HMDB0006528	C16513	DPA	0.01	0.31	1.55	0.63	1.99
	HMDB0001999	C06428	EPA	0.02	0.32	1.54	0.62	1.70
Organic acids	HMDB0000700	C01013	Hydroxypropionic acid	0.01	0.31	1.27	0.35	1.21
Fatty acids	HMDB0000673	C01595	Linoleic acid	0.05	0.44	1.39	0.47	1.54
Carnitines	HMDB0006469	NA	Linoleylcarnitine	0.01	0.31	1.40	0.49	2.16
Fatty acids	HMDB0000806	C06424	Myristic acid	0.01	0.31	1.61	0.69	1.76
	HMDB0000207	C00712	Oleic acid	0.02	0.32	1.45	0.54	1.86
Carnitines	HMDB0005065	NA	Oleylcarnitine	0.01	0.31	1.21	0.28	2.32
Fatty acids	HMDB0003229	C08362	Palmitoleic acid	0.02	0.31	1.53	0.61	1.62
	HMDB0000826	C16537	Pentadecanoic acid	0.03	0.42	1.51	0.60	1.51
Benzenoids	HMDB0000205	C00166	Phenylpyruvic acid	0.04	0.44	0.86	-0.22	0.85
Carnitines	HMDB0013128	NA	Valerylcarnitine	0.02	0.31	1.21	0.27	1.47
Organic acids	HMDB0000617	C01546	2-Furoic acid	0.00	0.00	148.12	7.21	2.10
Phenylpropanoic acids	HMDB0011743	NA	2-Phenylpropionate	0.01	0.04	2.89	1.53	1.26
Organic acids	HMDB0000357	C01089	3-Hydroxybutyric acid	0.04	0.20	0.56	-0.83	0.59
Fatty acids	HMDB0000555	NA	3-Methyladipic acid	0.05	0.22	0.95	-0.07	2.09
	HMDB0001043	C00219	Arachidonic acid	0.00	0.01	0.66	-0.60	2.11
	HMDB0000784	C08261	Azelaic acid	0.05	0.22	1.07	0.10	0.86
Organic acids	HMDB0001870	C00180	Benzoic acid	0.00	0.00	346.31	8.44	2.42
Bile acids	HMDB0000686	C17662	bUDCA	0.00	0.02	0.64	-0.64	1.37
SCFAs	HMDB0000039	C00246	Butyric acid	0.00	0.00	3.72	1.89	2.54
Carnitines	HMDB0002013	C02862	Butyrylcarnitine	0.00	0.02	0.55	-0.87	1.80
Bile acids	HMDB0000619	C00695	CA	0.02	0.16	1.42	0.51	1.27
Organic acids	HMDB0000072	C02341	Aconitic acid	0.00	0.01	1.37	0.46	0.76
	HMDB0000094	C00158	Citric acid	0.00	0.02	1.21	0.27	1.31
Carbohydrates	HMDB0000122	C00221	Glucose	0.05	0.22	1.10	0.14	0.75
Carnitines	HMDB0000651	NA	Decanoylcarnitine	0.01	0.06	0.52	-0.94	0.55
Amino acids	HMDB0000092	C01026	Dimethylglycine	0.00	0.03	1.27	0.35	0.90
Amino acids	HMDB0000112	C00334	GABA	0.01	0.05	1.17	0.23	0.46
	HMDB0000123	C00037	Glycine	0.04	0.19	1.18	0.23	1.07
Bile acids	HMDB0000637	C05466	GCDCA	0.00	0.00	6.42	2.68	2.30
Organic acids	HMDB0000115	C00160	Glycolic acid	0.03	0.18	1.26	0.33	1.03
Fatty acids	HMDB0000666	C17714	Heptanoic acid	0.03	0.19	1.30	0.38	1.07

Phenols	HMDB0000118	C05582	Homovanillic acid	0.00	0.01	1.26	0.33	2.40
Phenylpropanoic acids	HMDB0000764	C05629	Hydrocinnamic acid	0.00	0.03	2.71	1.44	1.23
	HMDB0000755	C03672	Hydroxyphenyllactic acid	0.00	0.01	1.44	0.53	2.20
Organic acids	HMDB0000193	C00311	Isocitric acid	0.05	0.22	1.39	0.48	0.65
	HMDB0000168	C00152	Asparagine	0.03	0.19	1.07	0.10	1.85
	HMDB0000719	C00263	Homoserine	0.04	0.19	1.20	0.26	1.41
	HMDB0000696	C00073	Methionine	0.00	0.04	1.23	0.30	1.59
	HMDB0000716	C00408	Pipelicolic acid	0.02	0.11	1.20	0.26	0.98
	HMDB0000158	C00082	Tyrosine	0.00	0.00	1.54	0.62	2.51
Carnitines	HMDB0000791	C02838	Octanoylcarnitine	0.03	0.19	0.75	-0.42	0.57
Phenylpropanoic acids	HMDB0000779	NA	Phenyllactic acid	0.00	0.04	2.81	1.49	1.44
SCFAs	HMDB0000237	C00163	Propionic acid	0.00	0.00	2.70	1.43	3.00
Bile Acids	HMDB0000951	C05465	TCDCa	0.00	0.00	11.04	3.47	1.80
	HMDB0000036	C05122	TCA	0.00	0.03	13.19	3.72	1.55
Validation set								
Carnitines	HMDB0000062	C00318	Carnitine	0.04	0.65	0.80	-0.31	1.73
	HMDB0001976	NA	DPA _n -6	0.04	0.65	1.79	0.84	2.00
	HMDB0003073	C06426	gamma-Linolenic acid	0.01	0.59	3.84	1.94	2.54
Amino acids	HMDB0000123	C00037	Glycine	0.03	0.65	0.85	-0.24	1.60
Peptides	HMDB0000721	NA	Glycylproline	0.01	0.59	0.85	-0.24	1.59
Amino acids	HMDB0000168	C00152	Asparagine	0.02	0.65	0.85	-0.24	1.41
	HMDB0000162	C00148	Proline	0.01	0.59	0.52	-0.94	1.53
	HMDB0006270	NA	Linoelaidic acid	0.00	0.06	2.15	1.10	2.62
	HMDB0002925	C03242	Dihomo-gamma-linolenic acid	0.04	0.80	1.65	0.72	1.39
	HMDB0001043	C00219	Arachidonic acid	0.05	0.80	1.42	0.51	1.59
Organic acids	HMDB0000700	C01013	Hydroxypropionic acid	0.04	0.80	0.47	-1.08	2.07
Amino acids	HMDB0000168	C00152	Asparagine	0.02	0.80	0.81	-0.31	2.66
	HMDB0000191	C00049	Aspartic acid	0.01	0.80	1.55	0.63	2.29
	HMDB0000158	C00082	Tyrosine	0.03	0.80	0.72	-0.47	2.51
	HMDB0000779	NA	Phenyllactic acid	0.03	0.80	0.60	-0.75	2.14
Organic acids	HMDB0000617	C01546	2-Furoic acid	0.00	0.02	148.81	7.22	1.66
Phenylpropanoic acids	HMDB0011743	NA	2-Phenylpropionate	0.00	0.02	13.73	3.78	1.90
Fatty acids	HMDB0001043	C00219	Arachidonic acid	0.02	0.17	0.69	-0.53	1.88
Organic acids	HMDB0001870	C00180	Benzoic acid	0.00	0.02	715.57	9.48	1.71
SCFAs	HMDB0000039	C00246	Butyric acid	0.00	0.05	7.84	2.97	1.80
	HMDB0000072	C02341	Aconitic acid	0.00	0.06	1.60	0.68	1.90
	HMDB0000094	C00158	Citric acid	0.00	0.02	1.54	0.62	2.32
Amino acids	HMDB0000092	C01026	Dimethylglycine	0.00	0.02	1.65	0.72	0.97
Bile acids	HMDB0000637	C05466	GCDCA	0.00	0.02	12.69	3.67	1.53
Phenols	HMDB0000118	C05582	Homovanillic acid	0.00	0.03	1.51	0.59	2.32
	HMDB0000764	C05629	Hydrocinnamic acid	0.00	0.03	7.97	2.99	1.88

	HMDB0000755	C03672	Hydroxyphenyllactic acid	0.03	0.25	1.63	0.70	2.10
Organic acids	HMDB0000193	C00311	Isocitric acid	0.00	0.06	2.32	1.21	1.29
	HMDB0000641	C00064	Glutamine	0.04	0.27	1.26	0.33	1.85
	HMDB0000684	C00328	Kynurenine	0.02	0.15	1.53	0.61	0.95
	HMDB0000158	C00082	Tyrosine	0.00	0.01	1.46	0.55	2.23
	HMDB0002931	NA	N-acetylserine	0.03	0.21	1.18	0.24	0.83
Fatty acids	HMDB0003229	C08362	Palmitoleic acid	0.03	0.25	1.60	0.68	1.07
	HMDB0000779	NA	Phenyllactic acid	0.03	0.25	20.79	4.38	1.84
Phenylpropanoic acids								
Benzoic acids	HMDB0002107	C01606	Phthalic acid	0.01	0.14	1.33	0.41	2.21
SCFAs	HMDB0000237	C00163	Propionic acid	0.01	0.08	4.41	2.14	2.19
Bile acids	HMDB0000951	C05465	TCDCa	0.00	0.00	9.63	3.27	1.75
	HMDB0000036	C05122	TCA	0.01	0.09	9.75	3.28	1.54

GCDCa: Glycochenodeoxycholic acid; TCA: Tricarboxylic acid; TCDCa: Taurochenodeoxycholic acid; NA: Not Applicable; DHA: Docosahexaenoic acid; DPA: Docosapentaenoic acid; EPA: Eicosapentaenoic acid; UDCA: Ursodeoxycholic acid; CA: Citric acid; GABA: Gamma-amino butyric acid.

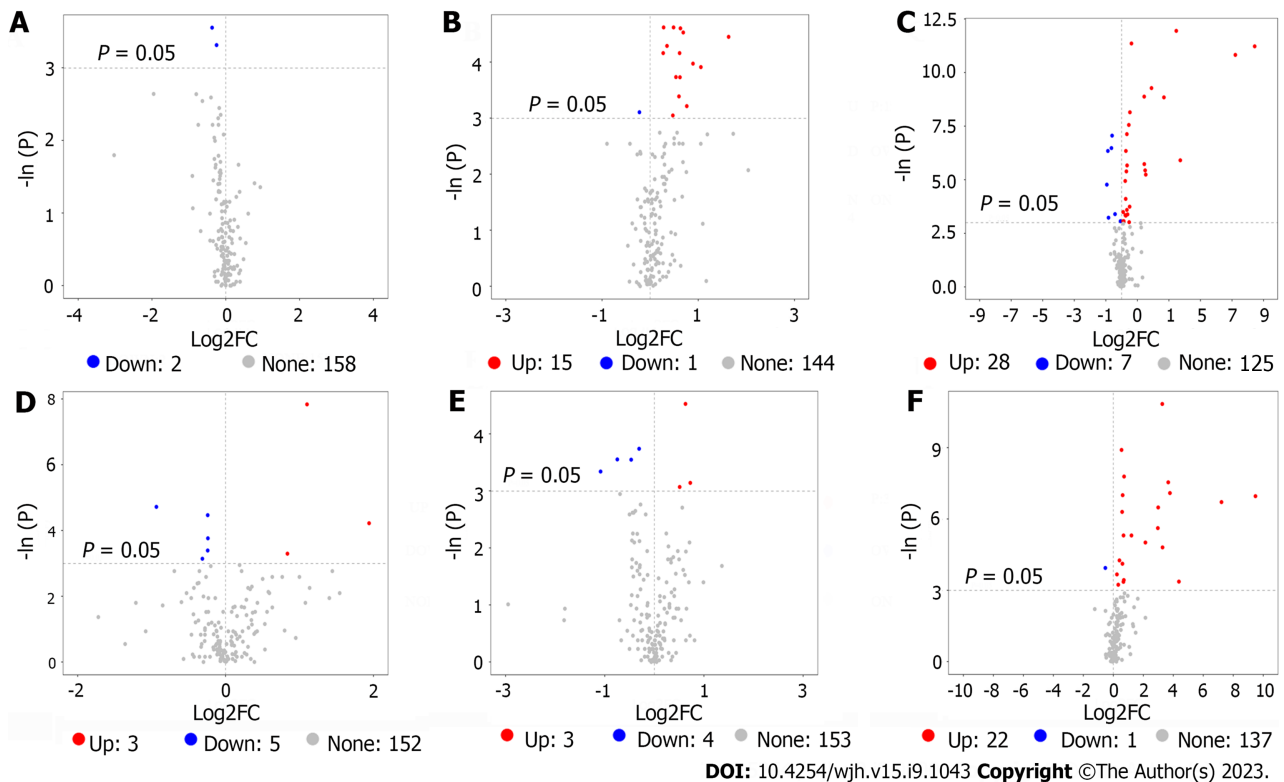
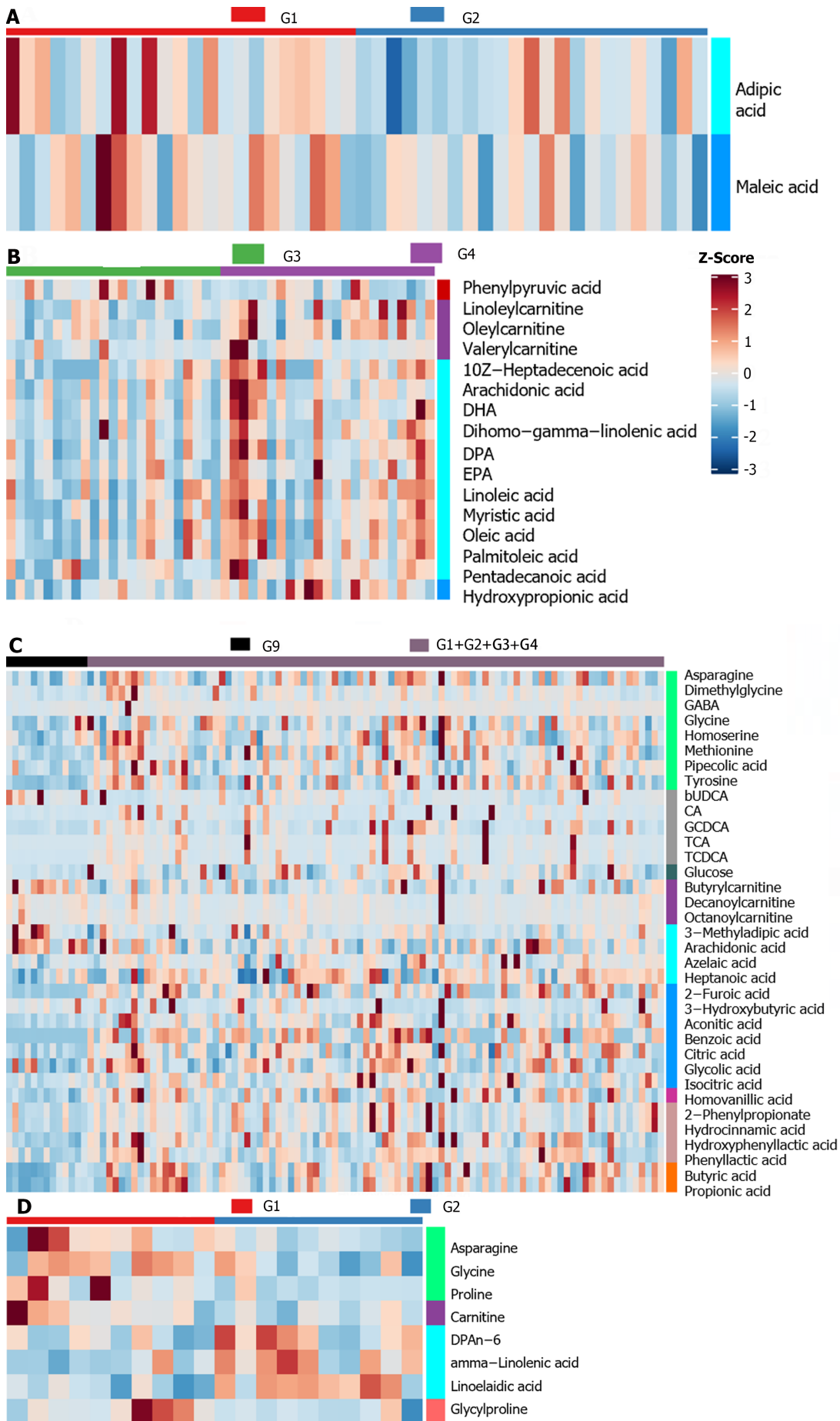


Figure 2 Volcano plot of serum metabolites. A: Volcano plot of entecavir responders (E-R) vs entecavir no-responders (E-N) (training set); B: Volcano plot of FuzhengHuayu tablet (FZHY) + entecavir responders (F-R) vs FZHY + entecavir no-responders (F-N) (training set); C: Volcano plot of patients vs volunteers (training set); D: Volcano plot of E-R vs E-N (validation set); E: Volcano plot of F-R vs F-N (validation set); F: Volcano plot of patients vs volunteers (validation set).

Metabolic pathways related to the selected metabolites in different sets

Both topological centrality (impact value > 0) and enrichment significance [$-\ln(p) > 2.99$, namely $P < 0.05$] were used to evaluate the analyses of enrichment and metabolic pathways for the selected potential metabolites. As shown in **Figure 4**, there were 2 pathways (butanoate metabolism, nicotinate and nicotinamide metabolism) (E-R vs E-N), 1 pathway (fatty acid biosynthesis) (F-R vs F-N), and 11 pathways (primary bile acid biosynthesis, nitrogen metabolism, butanoate metabolism, aminoacyl-tRNA biosynthesis, cyanoamino acid metabolism, phenylalanine metabolism, glycine, serine and threonine metabolism, glyoxylate and dicarboxylate metabolism, citrate cycle (TCA cycle), thiamine metabolism, alanine, aspartate and glutamate metabolism) (patients vs volunteers) in the training set (**Figure 4A-C**); and there were 6 pathways (aminoacyl-tRNA biosynthesis, cyanoamino acid metabolism, nitrogen metabolism, linoleic acid metabolism, thiamine



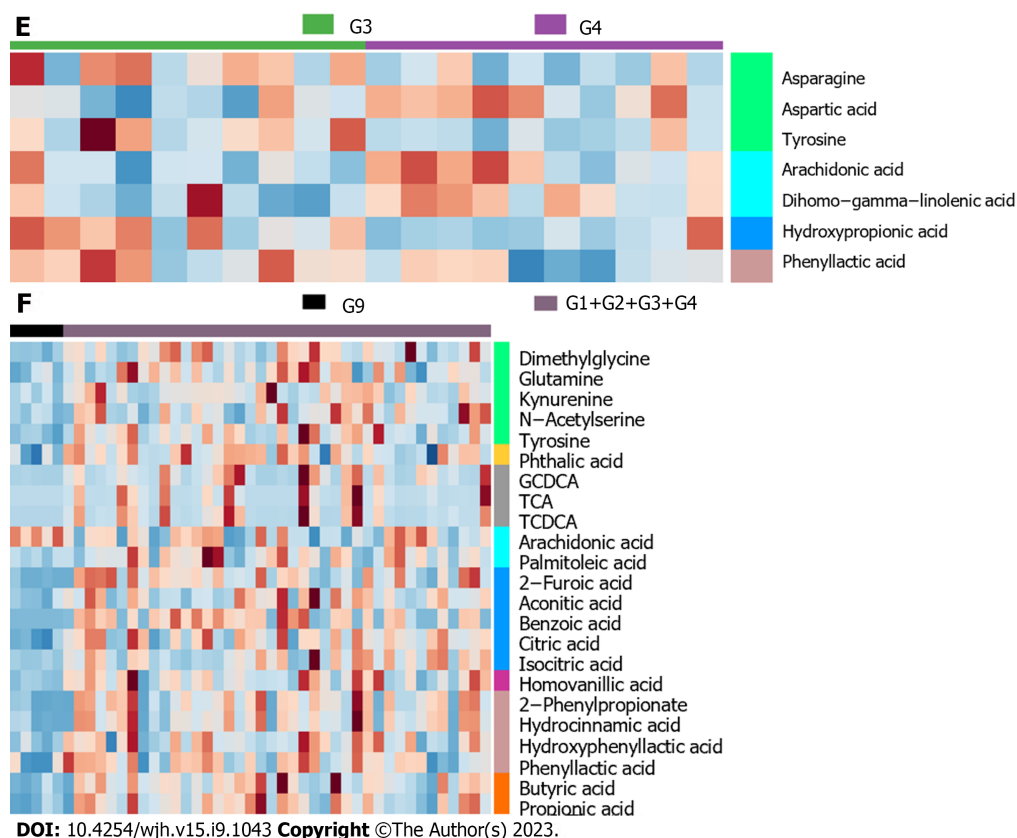


Figure 3 Heatmap of all the selected potential metabolites. A: Heatmap of entecavir responders (E-R) vs entecavir no-responders (E-N) (training set); B: Heatmap of FuzhengHuayu tablet (FZHY) + entecavir responders (F-R) vs FZHY + entecavir no-responders (F-N) (training set); C: Heatmap of patients vs volunteers (training set); D: Heatmap of E-R vs E-N (validation set); E: Heatmap of F-R vs F-N (validation set); F: Heatmap of patients vs volunteers (validation set). CA: Citric acid; GCDCA: Glycochenodeoxycholic acid; TCA: Tricarboxylic acid; TCDC A: Aurochenodeoxycholic acid; DHA: Docosahexaenoic acid; DPA: Docosapentaenoic acid; EPA: Eicosapentaenoic acid.

metabolism, alanine, aspartate and glutamate metabolism) (E-R vs E-N), 5 pathways (nitrogen metabolism, aminoacyl-tRNA biosynthesis, cyanoamino acid metabolism, alanine, aspartate and glutamate metabolism, beta-alanine metabolism) (F-R vs F-N), and 6 pathways (phenylalanine metabolism, primary bile acid biosynthesis, TCA cycle, tyrosine metabolism, ubiquinone and other terpenoid-quinone biosynthesis, nitrogen metabolism) (patients vs volunteers) in the validation set (Figure 4D-F).

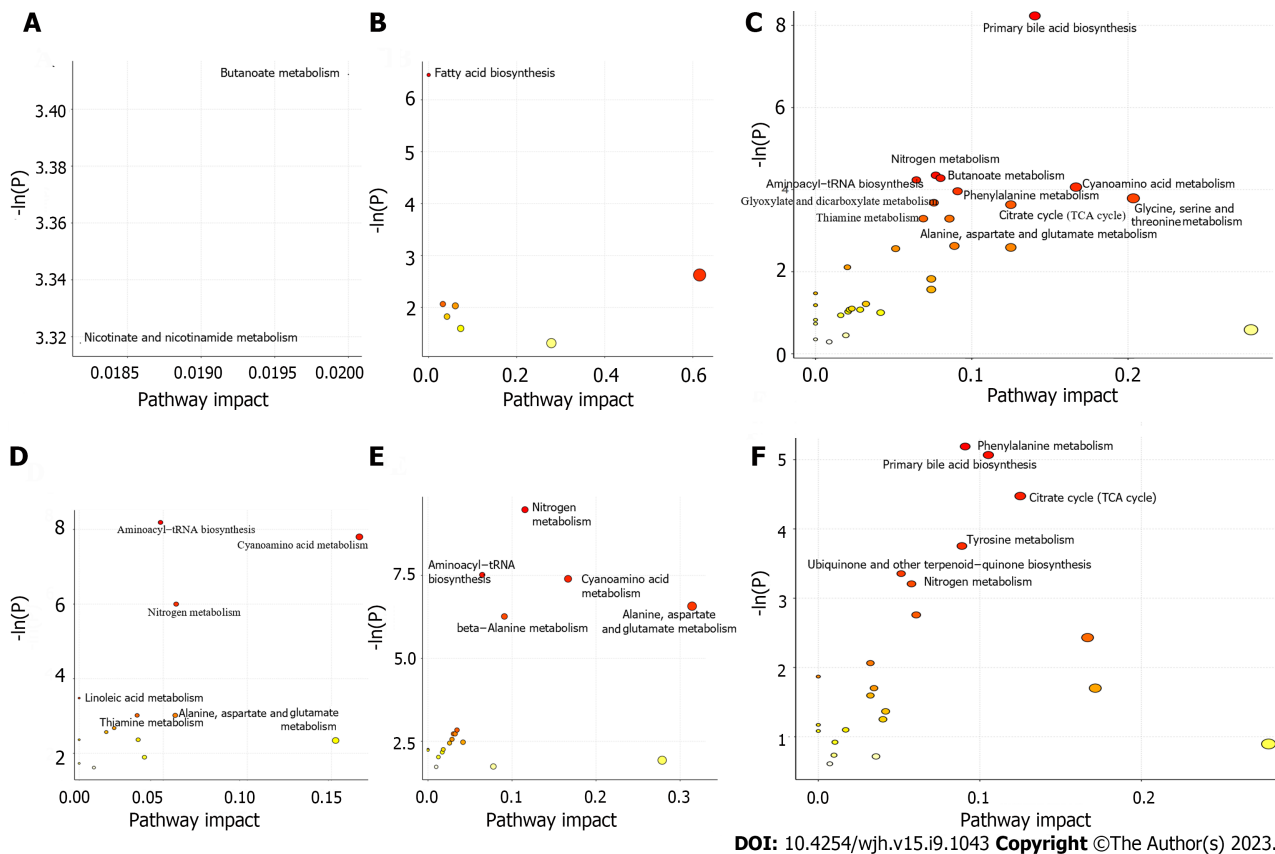
Selection of differential metabolites in different sets

In order to find differential metabolites from these selected potential metabolites, RF, SVM and Boruta analyses were conducted for each selected metabolite in sequence. And intersection of these potential metabolites in the three analyses can be found in Supplementary Figure 5. Specifically, there were Maleic acid and Adipic acid (E-R vs E-N), Hydroxypropionic acid, 10Z-heptadecenoic acid, and linoleylcarnitine (F-R vs F-N), tyrosine, benzoic acid, 2-Furoic acid, aconitic acid, and butyrylcarnitine (patients vs volunteers) in the training set while there were linoelaidic acid, gamma-linolenic acid, glycyproline, proline, asparagine, and carnitine (E-R vs E-N), hydroxypropionic acid, aspartic acid, dihomogamma-linolenic acid, and tyrosine (F-R vs F-N), dimethylglycine, citric acid, GCDCA, and 2-phenylpropionate (patients vs volunteers) in the validation set.

In the results of Boruta analysis (Figure 5), the metabolites marked as confirmed are the differential metabolites obtained by the final screening for subsequent model construction. As shown in Figure 5A-C, in addition to the above intersection metabolites, there were arachidonic acid, oleylcarnitine, and docosahexaenoic acid (F-R vs F-N), butyric acid, TCDC A, arachidonic acid, citric acid, and propionic acid (patients vs volunteers) confirmed in the training set. As shown in Figure 5D-F, in addition to the above intersection metabolites, there were TCDC A, benzoic acid, tyrosine, 2-Furoic acid, butyric acid, TCA, isocitric acid, hydrocinnamic acid, and propionic acid (patients vs volunteers) confirmed in the validation set.

Evaluation of model effects in different sets

In the training set, there were good sensitivity and specificity with the AUC value of 0.851 (F-R vs F-N) and 0.985 (patients vs volunteers) except for 0.733 (E-R vs E-N) (Figure 6A-C). In the validation set, there were good sensitivity and specificity with the AUC value of 1 (E-R vs E-N, patients vs volunteers) and 0.94 (F-R vs F-N) (Figure 6D-F). On the whole, the above AUC values of the two sets indicated good diagnostic capability in this study.



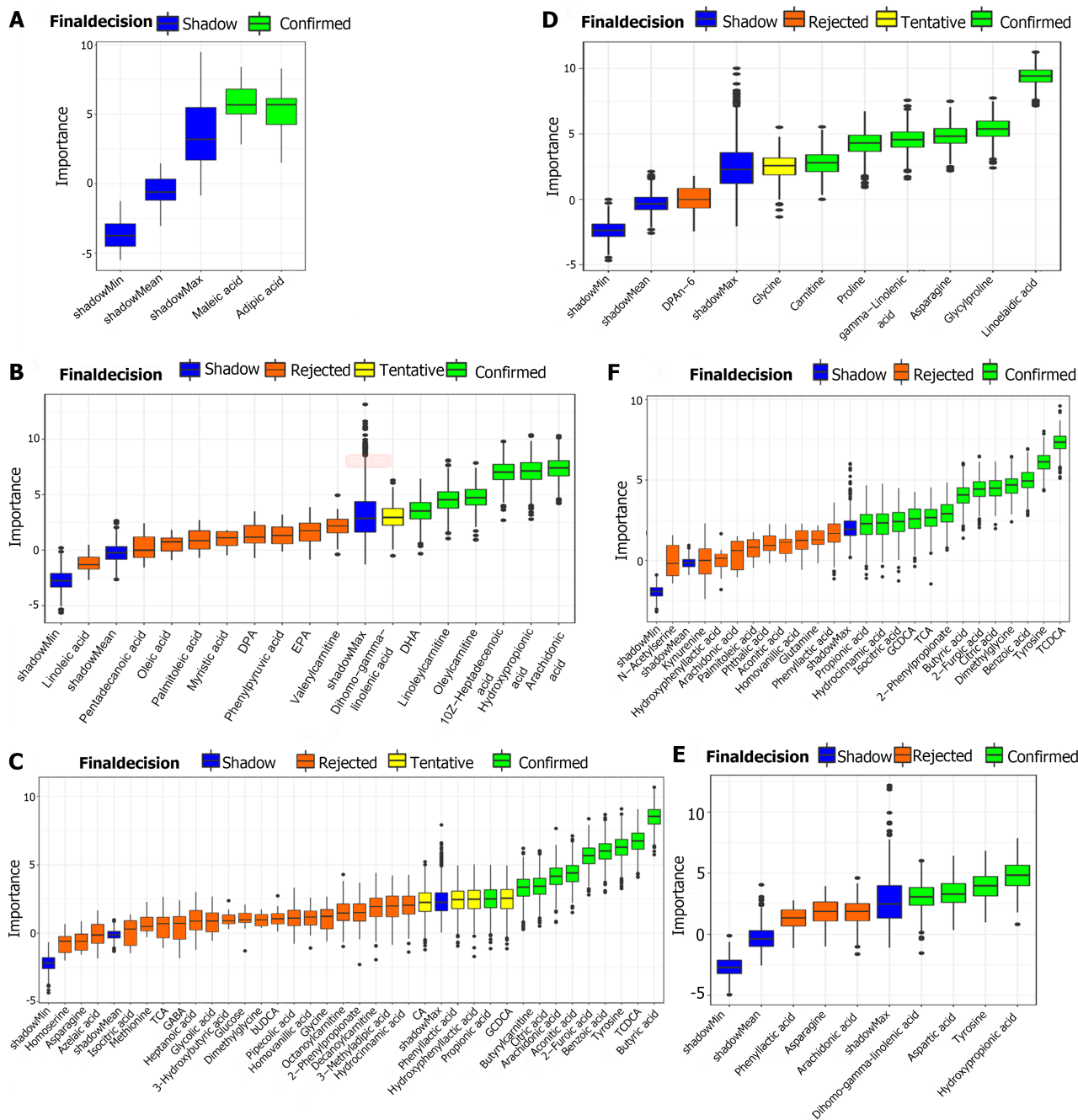
DOI: 10.4254/wjh.v15.i9.1043 Copyright ©The Author(s) 2023.

Figure 4 Bubbleplot of the selected metabolites pathways. A: Bubbleplot of entecavir responders (E-R) vs entecavir no-responders (E-N) (training set); B: Bubbleplot of FuzhengHuayu tablet (FZHY) + entecavir responders (F-R) vs FZHY + entecavir no-responders (F-N) (training set); C: Bubbleplot of patients vs volunteers (training set); D: Bubbleplot of E-R vs E-N (validation set); E: Bubbleplot of F-R vs F-N (validation set); F: Bubbleplot of patients vs volunteers (validation set). TCA: Tricarboxylic acid.

DISCUSSION

With the global prevalence of HBV-related liver fibrosis on the rise, precise targeting of the population that responds to entecavir or entecavir + FZHY is of paramount importance for improving clinical efficacy through precision treatment. Metabolomics serves as a valuable tool for biomarker discovery[18]. In this study, we employed HPLC-MS and advanced multivariate statistical modeling to predict the serum differential metabolites associated with interventions effectively reversing HBV-related liver fibrosis. Our findings revealed the involvement of 7 metabolic pathways (E-R *vs* E-N), including linoleic acid metabolism, aminoacyl-tRNA biosynthesis, cyanoamino acid metabolism, alanine, aspartate, and glutamate metabolism, nitrogen metabolism, butanoate metabolism, and nicotinate and nicotinamide metabolism. Similarly, 7 metabolic pathways (F-R *vs* F-N) were identified, encompassing linoleic acid metabolism, aminoacyl-tRNA biosynthesis, cyanoamino acid metabolism, alanine, aspartate, and glutamate metabolism, nitrogen metabolism, beta-alanine metabolism, and fatty acid biosynthesis. Furthermore, 3 metabolic pathways (patients *vs* volunteers) were noted, which included nitrogen metabolism, primary bile acid biosynthesis, and the TCA cycle. Regarding the intersection of differential metabolic pathways between the E-R *vs* E-N and F-R *vs* F-N groups, our study highlighted 4 common pathways: Linoleic acid metabolism, aminoacyl-tRNA biosynthesis, cyanoamino acid metabolism, and alanine, aspartate, and glutamate metabolism.

Regarding linoleic acid metabolism, a study suggested an inverse association between dietary linoleic acid intake and the risk of significant liver fibrosis, particularly emphasizing the ratio of unsaturated to saturated fatty acids[19]. Another clinical investigation demonstrated that specific alterations in linoleic acid metabolites could differentiate individuals with moderate alcohol-associated hepatitis from those with mild alcohol-associated liver disease among heavy drinkers. It is noteworthy that alcohol-associated liver diseases share common characteristics, spanning from steatosis to steatohepatitis, fibrosis, and cirrhosis[20]. Concerning aminoacyl-tRNA biosynthesis, an animal experiment revealed that Ganfule capsules could mitigate liver injury and liver fibrosis induced by bile duct ligation in mice. These effects were associated with the regulation and control of metabolic pathways, including glutamine metabolism, valine, leucine, and isoleucine biosynthesis, as well as aminoacyl-tRNA biosynthesis[21]. Furthermore, findings from a nonalcoholic fatty liver disease rat model indicated that metabolic disturbances primarily revolved around aminoacyl-tRNA biosynthesis, nitrogen metabolism, lipid metabolism, glyoxylate and dicarboxylate metabolism, and amino metabolism[22]. As for alanine, aspartate, and glutamate metabolism, a study aimed at investigating the role of the Wnt/ β -catenin signaling pathway and the enzyme l-glutaminase in liver fibrosis pathogenesis and the potential benefits of niclosamide in treating liver fibrosis. It was observed that the group of rats treated with niclosamide and CC cytokine ligand-4 exhibited significant reductions



DOI: 10.4254/wjh.v15.i9.1043 Copyright ©The Author(s) 2023.

Figure 5 Boxplot of all the differential metabolites. A: Boxplot of entecavir responders (E-R) vs entecavir no-responders (E-N) (training set); B: Boxplot of FuzhengHuayu tablet (FZHY) + entecavir responders (F-R) vs FZHY + entecavir no-responders (F-N) (training set); C: Boxplot of patients vs volunteers (training set); D: Boxplot of E-R vs E-N (validation set); E: Boxplot of F-R vs F-N (validation set); F: Boxplot of patients vs volunteers (validation set).

in TBIL, alanine transaminase, aspartate transaminase, β -catenin, l-hydroxyproline, and l-glutaminase activity. These findings led to the conclusion that Niclosamide protected rats against liver fibrosis by inhibiting the Wnt/ β -catenin pathway and glutaminolysis[23]. In summary, the metabolic pathways identified in this study are intricately linked to the initiation and progression of liver fibrosis.

The investigation into baseline differential metabolites for predicting the response to entecavir or entecavir + FZHY in HBV-related fibrotic livers has unveiled crucial insights with the potential to enhance tailored treatments for individuals. Notably, our findings indicated that specific differential metabolites, as mentioned earlier, were closely associated with the response to entecavir and entecavir + FZHY in HBV-related fibrotic livers. Furthermore, this study proposed that these baseline differential metabolites could be effectively combined with clinical parameters to enhance the precision of personalized treatment for patients grappling with HBV-related liver fibrosis. This approach holds the key to reducing the incidence of treatment failures stemming from inappropriate therapeutic interventions. Moreover, the insights gleaned from this research bear significant implications for the advancement of biomarker-guided precision medicine. These differential metabolites can potentially be employed to predict disease progression, select the most suitable treatment modalities, and monitor treatment outcomes among HBV patients. Additionally, this study provides a

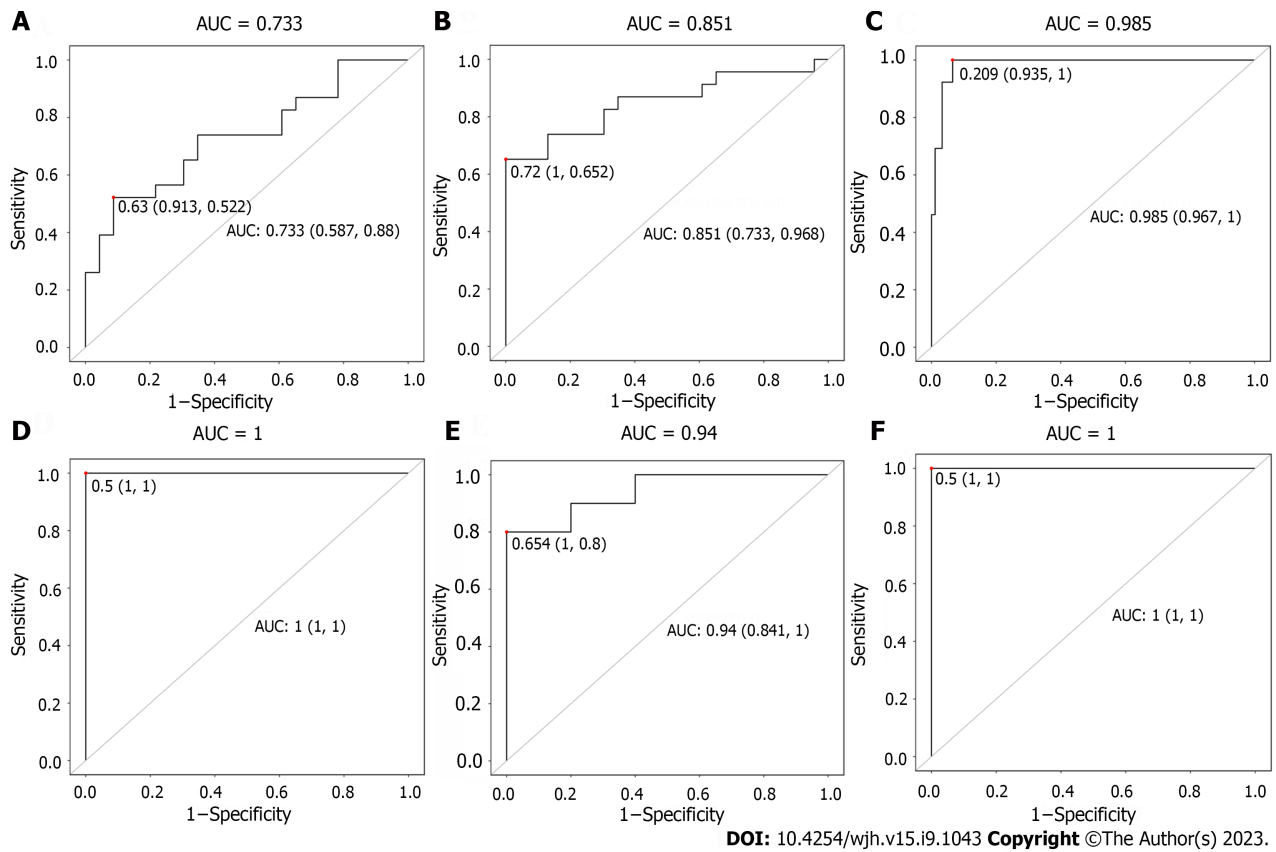


Figure 6 Receiver operating characteristic curve of all the differential metabolites. A: Receiver operating characteristic (ROC) curve of entecavir responders (E-R) vs entecavir no-responders (E-N) (training set); B: ROC curve of FuzhengHuayu tablet (FZHY) + entecavir responders (F-R) vs FZHY + entecavir no-responders (F-N) (training set); C: ROC curve of patients vs volunteers (training set); D: ROC curve of E-R vs E-N (validation set); E: ROC curve of F-R vs F-N (validation set); F: ROC curve of patients vs volunteers (validation set). AUC: Area under the curve.

foundation for the exploration of novel metabolites or biomarkers that might serve as superior predictors of the response to entecavir or entecavir + FZHY in HBV-related fibrotic livers. Ultimately, these findings contribute to an enhanced understanding of the molecular mechanisms underpinning HBV-related liver fibrosis and may offer opportunities to more accurately evaluate the efficacy of individualized treatments. By comprehending the intricate association between these differential metabolites and the response to entecavir and entecavir + FZHY, healthcare practitioners can fine-tune treatment options for each patient, thereby optimizing the effectiveness of HBV-related liver fibrosis therapy. Furthermore, the outcomes of this study can serve as a valuable resource for the development of future pharmacological treatments that target different pathways more effectively in combatting HBV-related liver fibrosis.

There are several noteworthy limitations in our study. Firstly, all of our sample sources were confined to China. This geographically limited distribution could potentially restrict the broader applicability of our therapeutic regimen. Secondly, there was no dedicated FZHY monotherapy group. Given that all participants included in our study were CHB patients, and the development of liver fibrosis in these individuals was directly or indirectly attributed to HBV infection, antiviral therapy was considered the foundational treatment. Administering FZHY as the sole treatment to HBV-related liver fibrosis patients would be ethically inconsistent with clinical standards. Consequently, we lacked an observation of the therapeutic efficacy of FZHY in isolation. In regard to the FZHY monotherapy group, for future research endeavors, it may be considered to further validate the identified differential metabolites and metabolic pathways by selecting alternative etiologies of liver fibrosis for validation or by investigating the distinctions between monotherapy and combination therapy in animal experiments. Thirdly, our study exclusively focused on patients with hepatitis B, and whether our conclusions can be extrapolated to the treatment of liver fibrosis arising from other causes necessitates further exploration. Lastly, due to the cross-sectional nature of our study, external reproducibility should be further evaluated through prospective studies.

CONCLUSION

In summary, through metabolomics analysis, we have identified 4 metabolic pathways and 7 differential metabolites from serum that accurately differentiated responders from no-responders in the treatment of HBV-related liver fibrosis. If validated in future studies, these metabolic pathways and differential metabolites will be useful in improving the curative effect of entecavir + FZHY and promoting the development of precision medicine.

ARTICLE HIGHLIGHTS

Research background

After receiving entecavir or combined with FuzhengHuayu tablet (FZHY) treatment, some sufferers with hepatitis B virus (HBV)-related liver fibrosis could achieve a histological improvement while the others may fail to improve even worsen. Serum metabolomics at baseline in these patients who were effective in treatment remain unclear.

Research motivation

The key significance of this cross-sectional study is to predict the serum metabolites of the treatment (entecavir or entecavir + FZHY) that effectively reversed HBV-related liver fibrosis.

Research objectives

We are about to explore serum differential metabolites and metabolic pathways at baseline in HBV-related liver fibrosis patients who are response to the treatments.

Research methods

A total of 132 patients with HBV-related liver fibrosis and 18 volunteers as healthy controls were recruited. First, all subjects were divided into training set and validation set. Second, the included patients were subdivided into entecavir responders (E-R), entecavir no-responders (E-N), FZHY + entecavir responders (F-R), and FZHY + entecavir no-responders (F-N) following the pathological histological changes after 48 wk' treatments. Then, serum samples of all subjects before treatment were tested by high-performance liquid chromatography-tandem mass spectrometry. Data processing was conducted using multivariate principal component analysis and orthogonal partial least squares discriminant analysis. Diagnostic tests of selected differential metabolites were used for Boruta analyses and logistic regression.

Research results

As for the intersection about differential metabolic pathways between the groups E-R *vs* E-N and F-R *vs* F-N, results showed that 4 pathways including Linoleic acid metabolism, aminoacyl-tRNA biosynthesis, cyanoamino acid metabolism, alanine, aspartate and glutamate metabolism were screened out. As for the differential metabolites, these 7 intersected metabolites including hydroxypropionic acid, tyrosine, citric acid, taurochenodeoxycholic acid, benzoic acid, 2-furoic acid, and propionic acid were selected.

Research conclusions

Our findings showed that 4 metabolic pathways and 7 differential metabolites have potential usefulness in clinical prediction of the response of entecavir or combined with FZHY on HBV fibrotic liver.

Research perspectives

It is of great theoretical and practical significance to prevent the transformation of liver fibrosis to cirrhosis or even hepatocellular carcinoma and reduce the social burden.

FOOTNOTES

Author contributions: Liu CH and Zhao ZM conceived and designed the study; Dai YK, Fan HN, Huang K and Sun X performed the experiment; Dai YK, Fan HN, Huang K and Sun X analyzed the data; Dai YK wrote the paper; Liu CH and Zhao ZM contributed to supervision; All authors approved the final manuscript as submitted.

Supported by National Science and Technology Major Project, No. 2014ZX10005001 and No. 2018ZX10302204; National Natural Science Foundation of China, No. 81730109 and No. 82274305; Shanghai Key Specialty of Traditional Chinese Clinical Medicine, No. shslczdk01201; China Postdoctoral Science Foundation, No. 2022M722162; Siming Youth Fund of Shuguang Hospital Affiliated to Shanghai University of Traditional Chinese Medicine, No. SGKJ-202104.

Institutional review board statement: This study was reviewed and approved by the Ethics Committee of Shuguang Hospital Affiliated to Shanghai University of Traditional Chinese Medicine.

Informed consent statement: All study participants or their legal guardian provided informed written consent about personal and medical data collection prior to study enrolment.

Conflict-of-interest statement: We have no financial relationships to disclose.

Data sharing statement: No additional data are available.

Open-Access: This article is an open-access article that was selected by an in-house editor and fully peer-reviewed by external reviewers. It is distributed in accordance with the Creative Commons Attribution NonCommercial (CC BY-NC 4.0) license, which permits others to

distribute, remix, adapt, build upon this work non-commercially, and license their derivative works on different terms, provided the original work is properly cited and the use is non-commercial. See: <https://creativecommons.org/licenses/by-nc/4.0/>

Country/Territory of origin: China

ORCID number: Yun-Kai Dai 0000-0002-1667-4670; Hai-Na Fan 0000-0002-5565-4875; Kai Huang 0000-0002-7294-8015; Xin Sun 0000 0001 5480 8062; Zhi-Min Zhao 0000-0002-0424-6089; Cheng-Hai Liu 0000-0002-1696-6008.

S-Editor: Qu XL

L-Editor: A

P-Editor: Cai YX

REFERENCES

- 1 **Roehlen N**, Crouchet E, Baumert TF. Liver Fibrosis: Mechanistic Concepts and Therapeutic Perspectives. *Cells* 2020; **9** [PMID: 32260126 DOI: 10.3390/cells9040875]
- 2 **Zhao J**, Qi YF, Yu YR. STAT3: A key regulator in liver fibrosis. *Ann Hepatol* 2021; **21**: 100224 [PMID: 32702499 DOI: 10.1016/j.aohp.2020.06.010]
- 3 **Inoue T**, Tanaka Y. Novel biomarkers for the management of chronic hepatitis B. *Clin Mol Hepatol* 2020; **26**: 261-279 [PMID: 32536045 DOI: 10.3350/cmh.2020.0032]
- 4 **Schweitzer A**, Horn J, Mikolajczyk RT, Krause G, Ott JJ. Estimations of worldwide prevalence of chronic hepatitis B virus infection: a systematic review of data published between 1965 and 2013. *Lancet* 2015; **386**: 1546-1555 [PMID: 26231459 DOI: 10.1016/S0140-6736(15)61412-X]
- 5 **Tang LSY**, Covert E, Wilson E, Kottlil S. Chronic Hepatitis B Infection: A Review. *JAMA* 2018; **319**: 1802-1813 [PMID: 29715359 DOI: 10.1001/jama.2018.3795]
- 6 **Dai YK**, Zhao ZM, Liu C. Treatment of Liver Fibrosis: A 20-Year Bibliometric and Knowledge-Map Analysis. *Front Pharmacol* 2022; **13**: 942841 [PMID: 35903335 DOI: 10.3389/fphar.2022.942841]
- 7 **Jung YK**, Yim HJ. Reversal of liver cirrhosis: current evidence and expectations. *Korean J Intern Med* 2017; **32**: 213-228 [PMID: 28171717 DOI: 10.3904/kjim.2016.268]
- 8 **Wu M**, Zhou Y, Qin SL, Lin LJ, Ping J, Tao Z, Zhang J, Xu LM, Wu J. Fuzheng Huayu Capsule Attenuates Hepatic Fibrosis by Inhibiting Activation of Hepatic Stellate Cells. *Evid Based Complement Alternat Med* 2020; **2020**: 3468791 [PMID: 32454856 DOI: 10.1155/2020/3468791]
- 9 **Dai YK**, Fan HN, Hu YH, Zhao ZM, Liu C. Comparison on different traditional Chinese medicine therapies for chronic hepatitis B liver fibrosis. *Front Pharmacol* 2022; **13**: 943063 [PMID: 36034853 DOI: 10.3389/fphar.2022.943063]
- 10 **Li ZX**, Zhao ZM, Liu P, Zheng QS, Liu CH. Treatment of HBV Cirrhosis with Fuzheng Huayu Tablet () and Entecavir: Design of a Randomized, Double-Blind, Parallel and Multicenter Clinical Trial. *Chin J Integr Med* 2021; **27**: 509-513 [PMID: 32572776 DOI: 10.1007/s11655-020-3257-6]
- 11 **Li C**, Li R, Zhang W. Progress in non-invasive detection of liver fibrosis. *Cancer Biol Med* 2018; **15**: 124-136 [PMID: 29951337 DOI: 10.20892/j.issn.2095-3941.2018.0018]
- 12 **Sebastiani G**. Serum biomarkers for the non-invasive diagnosis of liver fibrosis: the importance of being validated. *Clin Chem Lab Med* 2012; **50**: 595-597 [PMID: 22505554 DOI: 10.1515/cclm-2011-0850]
- 13 **Patel K**, Sebastiani G. Limitations of non-invasive tests for assessment of liver fibrosis. *JHEP Rep* 2020; **2**: 100067 [PMID: 32118201 DOI: 10.1016/j.jhepr.2020.100067]
- 14 **Amathieu R**, Triba MN, Goossens C, Bouchemal N, Nahon P, Savarin P, Le Moyec L. Nuclear magnetic resonance based metabolomics and liver diseases: Recent advances and future clinical applications. *World J Gastroenterol* 2016; **22**: 417-426 [PMID: 26755887 DOI: 10.3748/wjg.v22.i1.417]
- 15 **Terrault NA**, Lok ASF, McMahon BJ, Chang KM, Hwang JP, Jonas MM, Brown RS Jr, Bzowej NH, Wong JB. Update on prevention, diagnosis, and treatment of chronic hepatitis B: AASLD 2018 hepatitis B guidance. *Hepatology* 2018; **67**: 1560-1599 [PMID: 29405329 DOI: 10.1002/hep.29800]
- 16 **Zhao ZM**, Zhu CW, Huang JQ, Li XD, Zhang YX, Liang J, Zhang W, Zhang Y, Jiang XG, Zong YL, Zhang KJ, Sun KW, Zhang B, Lv YH, Xing HC, Xie Q, Liu P, Liu CH. Efficacy and safety of Fuzheng Huayu tablet on persistent advanced liver fibrosis following 2 years entecavir treatment: A single arm clinical objective performance criteria trial. *J Ethnopharmacol* 2022; **298**: 115599 [PMID: 35932973 DOI: 10.1016/j.jep.2022.115599]
- 17 **Ishak K**, Baptista A, Bianchi L, Callea F, De Groote J, Gudat F, Denk H, Desmet V, Korb G, MacSween RN. Histological grading and staging of chronic hepatitis. *J Hepatol* 1995; **22**: 696-699 [PMID: 7560864 DOI: 10.1016/0168-8278(95)80226-6]
- 18 **Shan D**, You L, Wan X, Yang H, Zhao M, Chen S, Jiang W, Xu Q, Yuan Y. Serum metabolomic profiling revealed potential diagnostic biomarkers in patients with panic disorder. *J Affect Disord* 2023; **323**: 461-471 [PMID: 36493940 DOI: 10.1016/j.jad.2022.12.004]
- 19 **Zhu T**, Lu XT, Liu ZY, Zhu HL. Dietary linoleic acid and the ratio of unsaturated to saturated fatty acids are inversely associated with significant liver fibrosis risk: A nationwide survey. *Front Nutr* 2022; **9**: 938645 [PMID: 35958259 DOI: 10.3389/fnut.2022.938645]
- 20 **Warner D**, Vatsalya V, Zirnheld KH, Warner JB, Hardesty JE, Umhau JC, McClain CJ, Maddipati K, Kirpich IA. Linoleic Acid-Derived Oxylipins Differentiate Early Stage Alcoholic Hepatitis From Mild Alcohol-Associated Liver Injury. *Hepatol Commun* 2021; **5**: 947-960 [PMID: 34141982 DOI: 10.1002/hep4.1686]
- 21 **Ke C**, Gao J, Tu J, Wang Y, Xiao Y, Wu Y, Liu Y, Zhou Z. Ganfule capsule alleviates bile duct ligation-induced liver fibrosis in mice by inhibiting glutamine metabolism. *Front Pharmacol* 2022; **13**: 930785 [PMID: 36278176 DOI: 10.3389/fphar.2022.930785]
- 22 **Zhu N**, Huang S, Zhang Q, Zhao Z, Qu H, Ning M, Leng Y, Liu J. Metabolomic Study of High-Fat Diet-Induced Obese (DIO) and DIO Plus CCl(4)-Induced NASH Mice and the Effect of Obeticholic Acid. *Metabolites* 2021; **11** [PMID: 34200685 DOI: 10.3390/metabo11060374]

- 23 **El-Ashmawy NE**, Al-Ashmawy GM, Fakher HE, Khedr NF. The role of WNT/ β -catenin signaling pathway and glutamine metabolism in the pathogenesis of CCl₄-induced liver fibrosis: Repositioning of niclosamide and concerns about lithium. *Cytokine* 2020; **136**: 155250 [PMID: 32882667 DOI: [10.1016/j.cyto.2020.155250](https://doi.org/10.1016/j.cyto.2020.155250)]



Published by **Baishideng Publishing Group Inc**
7041 Koll Center Parkway, Suite 160, Pleasanton, CA 94566, USA
Telephone: +1-925-3991568
E-mail: bpgoffice@wjgnet.com
Help Desk: <https://www.f6publishing.com/helpdesk>
<https://www.wjgnet.com>

